Indian Journal of Chemistry
Vol. 56A, January 2017, pp. 9-20

# DFT study for radical capture by mitochondria oxidotoxin protective ionic and non-ionic amphiphilic α-phenyl-N-*t*-butyl nitrone derivatives

Sutapa Mandal & Nivedita Acharjee*

Department of Chemistry, Durgapur Government College, Jawahar Lal Nehru Rd, Durgapur 713 214, Dist. Burdwan, West Bengal, India

Email: nivchem@gmail.com; nivedita_acharjee@rediffmail.com

*Received 6 April 2016; revised and accepted 26 December 2016*

DFT analysis for radical capture by a series of biologically active amphiphilic α-phenyl-N-*t*-butyl nitrone derivatives has been reported in the present study. A detailed analysis of global and local reactivity descriptors has been presented from both natural and electrostatic based charges. Reactivities of the investigated nitrones for radical capture have been compared by interaction energy calculations derived from a perturbative orbital independent theoretical model. The transition states for radical attacks have been located and the activation barriers for radical capture are calculated. The *cis* attack is found to be energetically favored in each case. Finally, the hyperfine splitting constants have been computed and compared with the reported experimental findings.

**Keywords:** Theoretical chemistry, Density functional calculations, Interaction energy, Transition state, Radical capture, Activation energy, Nitrones

The most critical pathophysical factor to consider in an aging brain is the decreasing efficiency of antioxidant systems due to progressive age-associated cellular damage. Nitrone moiety can act as spin trap and therefore has potential in the treatment of neurogenerative diseases and prolongation of life span. *C*-phenyl-*N*-*t*-butyl nitrone (PBN) has been extensively investigated and numerous experimental neuroprotective effects have been ascribed to this compound[1-4]. Despite the wide applicability of PBN in various animal models, several problems emerge with regard to its clinical administration[5]. One of these difficulties is related to its limited stability. It can decompose to N-*t*-butylhydroxylamine[6] and also liberate NO. Moreover, PBN adducts can be additionally metabolized by $P_{450}$ isoforms[7]. Modification of either the aromatic or N-terminal moieties of PBN to improve its bioavailability and change the hydrophilic-lipophilic balance has been reported[8-10]. Polidori *et al.*[11] developed new amphiphilic PBN derivative spin traps and concluded that the amphiphilic character is the most important parameter in terms of biological efficiency. The importance of amphiphilicity was further tuned by Durand and coworkers[12] by synthesis of new hydrophilic, amphiphilic and lipophilic analogues of PBN. Polidori *et al.*[11] have also reported the hyperfine splitting constants for methyl radical addition to these nitrones.

With this in view, the present report aims to investigate methyl radical addition to these ionic and non-ionic amphiphilic PBN derivatives in terms of DFT level of theory. Twelve nitrones have been selected for the present investigation including PBN designated as nitrone **1** throughout this report (Fig. 1). Nitrones **2**, **3** and **4** involve a lactobionyl moiety attached to the aromatic ring of PBN with the hydro- or perfluorocarbon chains containing a thioether or amide bond at the N-terminal. For nitrones **5**, **6**, **7** and **8**, carboxylate and for **12**, trimethylamine group is introduced in the aromatic ring. MitoPBN or nitrone **9** is a well known mitochondria targeted spin trap and has been discussed in several reports[13-15] for the prevention of mitochondrial lipid peroxidation and oxidative damage. Carnitine-derivative nitrone **11** has been reported[16] to prevent the oxidative stress associated with aging.

The present study has been sectioned into three theoretical aspects. DFT based reactivity descriptors[17-21] have been successfully employed to interpret wide variety of reactions. Unfortunately, there are very limited reports which address their applicability for nitrone radical reactions to the best of our knowledge.

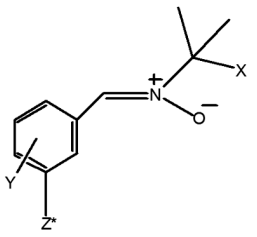

| | X | Y |
|---|---|---|
| **1** | $CH_3$ | H |
| **2** | $CH_2NHCOC_7H_{15}$ | *p*- |
| **3** | $CH_2SC_8H_{17}$ | *p*- |
| **4** | $CH_2SC_2H_4C_6F_{13}$ | *p*- |
| **5** | $CH_2NHCOC_7H_{15}$ | *p*-COONa |
| **6** | $CH_2SC_8H_{17}$ | *p*-COONa |
| **7** | $CH_2SC_2H_4C_6F_{13}$ | *p*-COONa |
| **8** | $CH_2OCONHC_7H_{15}$ | *p*-COONa |
| **9** | $CH_3$ | *p*-$OCH_2CH_2P(Ph)_3$ |
| **10** | $CH_2NHCOC_7H_{15}$ | *o*-$OCH_2CH_3$ |
| **11*** | $CH_3$ | *p*-$OC_{12}H_{25}$ |
| **12** | $CH_2SC_8H_{17}$ | *p*-$N(CH_3)_3$ |

*Z= $OC_6H_{12}COOCH(CH_2NMe_3)(CH_2COOC_8H_{17})$ for **11** and H for other nitrones

Fig. 1—Ionic and non-ionic amphiphilic α-phenyl-N-*t*-butyl nitrone derivatives (**1**-**12**).

In the present study, DFT based reactivity indices have been calculated both from NPA[22] and MK[23] analyses. Subsequently, a critical analysis of whether these descriptors can be used to predict the reactivities in the radical reactions of the investigated nitrones has been attempted. In the second section, the interaction energies for nitrone-radical attack have been calculated from both NPA and MK calculations. The final phase of study is focused on locating the transition states for these reactions and determining the activation and reaction energies for both *cis* and *trans* attack. The extent of bond formation in the transition states and radical adducts have been predicted by analysis of wiberg bond indices and atom-atom overlap weighted NAO bond orders. The standard orientations and charges are collected in Tables S1-S96 (Supplementary Data)

## Theory and Computational Methods

Electronic chemical potential ($\mu$)[17], chemical hardness ($\eta$)[20], ionization potential ($I$)[24], electron affinity ($A$)[24], global electrophilicity index ($\omega$)[21], global softness (S)[25], Fukui functions ($f_k^+$, $f_k^-$, $f_k^0$)[26, 27], local electrophilicity index ($\omega_k$)[25-27] and the local softnesses ($s^+$, $s^-$, $s^0$)[21] were calculated from the standard equations available in literature.

The interaction energies were calculated[28] from density functional theory (DFT) as:

$$\Delta E_{int} = \Delta E_\upsilon + \Delta E_\mu \quad \text{... (1)}$$

where $\Delta E_\upsilon$ and $\Delta E_\mu$ are the energy changes at constant external potential and constant chemical potential respectively and are written as:

$$\Delta E_\upsilon \approx -1/2\ [\{S_A S_B\ [\mu_A - \mu_B]^2\}/\{S_A + S_B\}] \quad \text{... (2)}$$

$$\Delta E_\mu \approx -1/2\ [\lambda/\{S_A + S_B\}] \quad \text{... (3)}$$

When we invoke the local viewpoint of one reactant, $\Delta E_\upsilon$, and $\Delta E_\mu$ in terms of condensed Fukui function $f_k$ become:

$$\Delta E_\upsilon \approx -1/2\ [\{S_A S_B f_k\ [\mu_A - \mu_B]^2\}/\{S_A f_k + S_B\}] \quad \text{... (4)}$$

$$\Delta E_\mu \approx -1/2\ [\lambda/\{f_k S_A + S_B\}] \quad \text{... (5)}$$

The interaction energy $(\Delta E_{int})^k{}_A$ can be rewritten in shorthand notation as:

$$(\Delta E_{int})^k{}_A \approx \Delta E_\upsilon + \lambda\ \Delta E'_\mu \text{ with } \Delta E'_\mu = \Delta E_\mu\ (\lambda = 1) \quad \text{... (6)}$$

The parameter $\lambda$ has been related to the deviation of total softness of interacting system AB from the sum of the softnesses of individual systems A and B. It has been defined somewhat arbitrarily in the literature[29-31]. In the present study, following the work of Mendez *et al.*[28] it has been initially assumed here that $\lambda$ is close to 1 and $\Delta E_\mu$ is much more important than $\Delta E_\upsilon$.

The geometries have been optimized by Density Functional Theory with Becke's[32] three-parameter hybrid exchange functional in combination with the gradient-corrected correlation functional of Lee, Yang, and Parr[33] (B3LYP) using 6-31G(d) basis set. This basis set has been reported to provide reliable results for nitrones. The stationary points were characterized through vibrational frequency analysis

done at 298.15 K at the DFT/B3LYP/6-31G(d) level. All the stationary points were definitely identified for minima (number of imaginary frequencies = 0) or transition states (number of imaginary frequencies = 1). Intrinsic reaction coordinate (IRC) calculations were performed to verify that the energy curve connecting the optimized reactants and the products passes through the correct and the lowest TS which must be a first-order saddle point. The electron affinity and ionization potential have been obtained at similar level using UB3LYP theory for the anion and cation. The geometries of the neutral species were used to calculate the electronic structure of the charged species in order to fulfill the demand for constant external potential. The electronic populations were computed from natural population analysis[22] and also by the charges derived from the electrostatic potential according to Merz-Kollman[23] algorithm. Solvent effects in water were considered at PCM/DFT/B3LYP/6-31G(d) level of theory from single-point energy calculations at the optimized gas phase geometries. All calculations were carried out using Gaussian 2003[34] set of programs.

## Results and Discussion

### DFT based reactivity indices

DFT calculated global properties of nitrones **1**-**12** have been listed in Table 1. The optimized geometries of nitrones and the radical adducts are shown in Fig. 2. The electronic chemical potentials of nitrones **9** (μ = −0.215 au) and **12** (μ = −0.226 au) are least in the series. It is worth mentioning in this context that nitrones **9** and **12** contain $PPh_3$ and $NMe_3$ groups in the *C*- phenyl substituent chain of the nitrone which is influencing the electron demand character of the nitrone moiety. This is also reflected in their highest global electrophilicities (3.068 eV for **9** and 2.907 eV for **12**) and the potential of ionization (*I* = 8.626 eV for **9** and *I* = 9.741 eV for **12**). Nitrones **1**-**8**, **10** and **11** with ω values ranging from 0.628 eV to 1.095 eV can be classified as moderate electrophiles according to the absolute scale of electrophilicity index[35]. Nitrones **9** and **12** with ω values of 3.068 eV to 2.907 eV can be classified as strong electrophiles. The charge transfer directions are generally predicted by a comparative analysis of the electronic chemical potential values of the substrate and the radical. In the present study, the electronic chemical potentials of nitrones **1**-**8, 10** and **11** are greater than that of methyl radical (μ = -0.146 au). This predicts the charge transfer direction from the nitrones to the radical. Contrary to the series, μ of methyl radical is greater than that of the nitrones **9** (μ = −0.215 au) and **12** (μ = −0.226 au). This predicts the direction of charge transfer from the radical to the nitrones **9** and **12** direction. The global electrophilicity indices of all the nitrones are either comparable or greater than that of the radical. This is in contrast to the electronic chemical potential values. Therefore, analysis of the local properties is required to obtain a rationalized approach.

Table 1—DFT/B3LYP/6-31G(d) calculated global properties of nitrones (**1**-**12**)

| Nitrone | μ (au) | η (au) | S (au) | ω (eV) | IP (eV) |
|---|---|---|---|---|---|
| **1** | -0.122 | 0.289 | 1.730 | 0.707 | 7.238 |
| **2** | -0.121 | 0.265 | 1.887 | 0.752 | 6.884 |
| **3** | -0.120 | 0.262 | 1.908 | 0.748 | 6.830 |
| **4** | -0.125 | 0.262 | 1.908 | 0.811 | 6.966 |
| **5** | -0.139 | 0.240 | 2.083 | 1.095 | 7.047 |
| **6** | -0.135 | 0.234 | 2.136 | 1.060 | 6.857 |
| **7** | -0.137 | 0.238 | 2.101 | 1.073 | 6.966 |
| **8** | -0.139 | 0.240 | 2.083 | 1.095 | 7.047 |
| **9** | -0.215 | 0.205 | 2.439 | 3.068 | 8.626 |
| **10** | -0.115 | 0.272 | 1.838 | 0.661 | 6.830 |
| **11** | -0.123 | 0.328 | 1.524 | 0.628 | 7.809 |
| **12** | -0.226 | 0.239 | 2.092 | 2.907 | 9.741 |

Table 2 lists the local properties of the investigated nitrones. The availability of DFT based reactivity descriptor reports for radical reactions are limited in literature[36]. The local HSAB principle points out that bond formation is preferable between the atom pair with the closest softness. On the other hand, Ponti's procedure[37] predicts that the softest between the two sites should be the most preferred site of attack. For the present study, Fukui functions for radical attack, $f_k^0$ and the local softness for radical attack, $s^o$, have been calculated following NPA and Merz-Kollman (MK) procedures. Fukui function calculated for radical attack $f_k^0$ at O1 is greater than that of C3 for all the nitrones from NPA calculations. However, MK results indicate greater $f_k^0$ at C3 compared to O1 except nitrone **9**.

NPA calculations further predict greater $s^o$ at O1 compared to C3 of the nitrones. On the contrary, $s^o$ of C3 is more than O1 by MK analysis for each nitrone except **9**. Experimentally, radical attack to nitrones takes place at C3. This suggests that DFT based reactivity studies from MK calculations perform better than the NPA system for radical reactions.

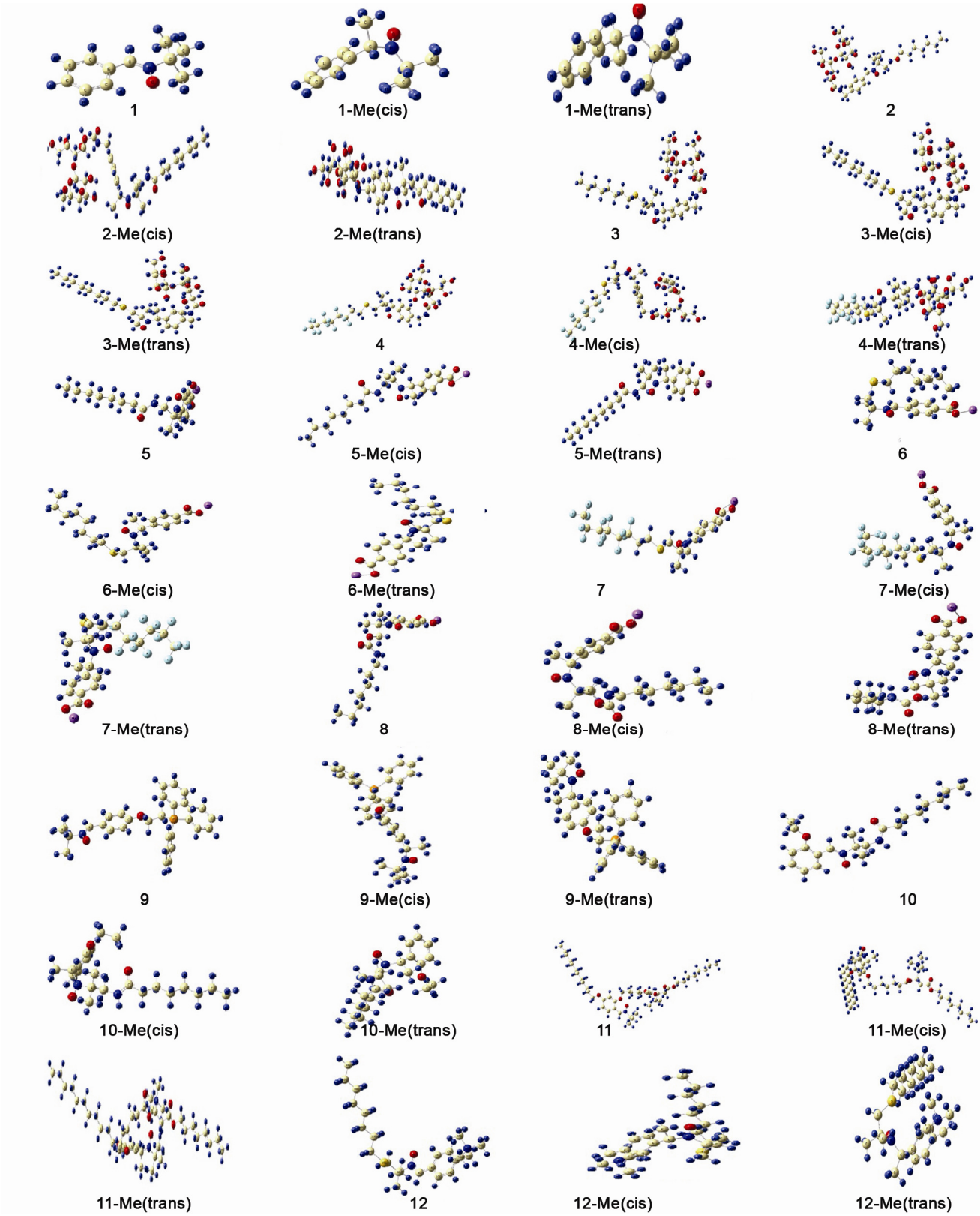


Fig. 2—DFT/B3LYP/6-31G(d) optimized nitrones and adducts.

Table 2—DFT/B3LYP/6-31G(d) calculated local properties of nitrones **1**-**12**

| Nitrone | k | $f_k^+$ | $f_k^-$ | $f_k^0$ | $s^+$(au) | $s^-$(au) | $s^0$(au) |
|---|---|---|---|---|---|---|---|
| | | | | NPA | | | |
| **1** | $O_1$ | 0.125 | 0.284 | 0.205 | 0.216 | 0.491 | 0.355 |
| | $C_3$ | 0.129 | 0.153 | 0.141 | 0.223 | 0.265 | 0.244 |
| **2** | $O_1$ | 0.111 | 0.222 | 0.167 | 0.230 | 0.461 | 0.346 |
| | $C_3$ | 0.110 | 0.124 | 0.117 | 0.223 | 0.257 | 0.240 |
| **3** | $O_1$ | 0.110 | 0.190 | 0.150 | 0.210 | 0.363 | 0.287 |
| | $C_3$ | 0.110 | 0.109 | 0.110 | 0.210 | 0.208 | 0.209 |
| **4** | O1 | 0.099 | 0.205 | 0.152 | 0.189 | 0.391 | 0.290 |
| | C3 | 0.105 | 0.110 | 0.108 | 0.200 | 0.210 | 0.205 |
| **5** | O1 | 0.052 | 0.239 | 0.146 | 0.108 | 0.498 | 0.303 |
| | C3 | 0.021 | 0.115 | 0.068 | 0.044 | 0.240 | 0.142 |
| **6** | O1 | 0.042 | 0.234 | 0.138 | 0.090 | 0.500 | 0.295 |
| | C3 | 0.026 | 0.107 | 0.067 | 0.056 | 0.229 | 0.143 |
| **7** | O1 | 0.042 | 0.245 | 0.144 | 0.088 | 0.515 | 0.302 |
| | C3 | 0.027 | 0.119 | 0.073 | 0.057 | 0.250 | 0.154 |
| **8** | O1 | 0.050 | 0.234 | 0.142 | 0.104 | 0.487 | 0.296 |
| | C3 | 0.021 | 0.118 | 0.070 | 0.044 | 0.246 | 0.145 |
| **9** | O1 | 0.012 | 0.259 | 0.136 | 0.029 | 0.632 | 0.331 |
| | C3 | 0.008 | 0.141 | 0.075 | 0.020 | 0.344 | 0.182 |
| **10** | O1 | 0.115 | 0.237 | 0.176 | 0.211 | 0.436 | 0.324 |
| | C3 | 0.126 | 0.115 | 0.121 | 0.232 | 0.211 | 0.222 |
| **11** | O1 | 0.126 | 0.224 | 0.175 | 0.192 | 0.341 | 0.267 |
| | C3 | 0.215 | 0.098 | 0.157 | 0.328 | 0.149 | 0.239 |
| **12** | O1 | 0.102 | 0.111 | 0.107 | 0.213 | 0.232 | 0.223 |
| | C3 | 0.042 | 0.106 | 0.074 | 0.088 | 0.222 | 0.155 |
| | | | | MK | | | |
| **1** | $O_1$ | 0.161 | 0.239 | 0.200 | 0.279 | 0.413 | 0.346 |
| | $C_3$ | 0.363 | 0.184 | 0.274 | 0.628 | 0.318 | 0.474 |
| **2** | $O_1$ | 0.143 | 0.190 | 0.167 | 0.297 | 0.394 | 0.346 |
| | $C_3$ | 0.308 | 0.169 | 0.239 | 0.639 | 0.351 | 0.495 |
| **3** | $O_1$ | 0.137 | 0.163 | 0.150 | 0.261 | 0.311 | 0.286 |
| | $C_3$ | 0.285 | 0.139 | 0.212 | 0.544 | 0.265 | 0.405 |
| **4** | O1 | 0.124 | 0.175 | 0.150 | 0.237 | 0.334 | 0.286 |
| | C3 | 0.267 | 0.144 | 0.206 | 0.509 | 0.275 | 0.392 |
| **5** | O1 | 0.103 | 0.199 | 0.151 | 0.215 | 0.415 | 0.315 |
| | C3 | 0.316 | 0.131 | 0.224 | 0.658 | 0.273 | 0.466 |
| **6** | O1 | 0.059 | 0.188 | 0.124 | 0.126 | 0.402 | 0.264 |
| | C3 | 0.295 | 0.093 | 0.194 | 0.630 | 0.199 | 0.415 |
| **7** | O1 | 0.072 | 0.205 | 0.139 | 0.151 | 0.431 | 0.291 |
| | C3 | 0.259 | 0.150 | 0.205 | 0.544 | 0.315 | 0.430 |
| **8** | O1 | 0.095 | 0.194 | 0.145 | 0.198 | 0.404 | 0.301 |
| | C3 | 0.231 | 0.143 | 0.187 | 0.481 | 0.298 | 0.390 |
| **9** | O1 | 0.011 | 0.218 | 0.115 | 0.027 | 0.532 | 0.280 |
| | C3 | 0.009 | 0.165 | 0.087 | 0.022 | 0.402 | 0.212 |
| **10** | O1 | 0.145 | 0.202 | 0.174 | 0.267 | 0.371 | 0.319 |
| | C3 | 0.319 | 0.131 | 0.225 | 0.586 | 0.241 | 0.414 |
| **11** | O1 | 0.136 | 0.173 | 0.155 | 0.207 | 0.264 | 0.236 |
| | C3 | 0.363 | 0.128 | 0.246 | 0.553 | 0.195 | 0.374 |
| **12** | O1 | 0.126 | 0.087 | 0.107 | 0.264 | 0.182 | 0.223 |
| | C3 | 0.165 | 0.078 | 0.122 | 0.345 | 0.163 | 0.254 |

In this context, it is worth mentioning that Chandra and Nguyen[36] critically analyzed the use of DFT-based reactivity descriptors for rationalizing radical reactions. The authors suggested that a particular difficulty in correlating the local softness for radical attack ($s^0$) likely arises from the fact that this quantity is not well defined. The local softness for nucleophilic ($s^+$) and electrophilic ($s^-$) attacks has a clear chemical meaning. However, the local softness for radical attack, defined as the average of $s^+$ and $s^-$ values is ambiguous. With this in mind, it has been attempted in the present study to calculate the interaction energies of the methyl radical attack to the investigated nitrones and obtain a more accurate prediction.

**Interaction energies**

Mendez *et al.*[38] reported that the interaction energies calculated between alkenes and carbenes are most favorable with parameters that reflect mutual electron donation, reflecting the simultaneous acidity and basicity of carbenes and alkenes. In the present study, the interaction energies were calculated from both natural (NPA) and electrostatic (MK) charge based analyses. A perturbative orbital independent theoretical model has been utilized[28] for the present study in line with our previous investigations of dipolar cycloadditions[39, 40].

Let us invoke the global viewpoint initially. $\Delta E_\upsilon$ and $\Delta E'_\mu$ values are calculated and listed in Table 3. The global interaction energies can be compared to predict the relative reactivities of different nitrones towards the radical attack. The interaction energy trend is as follows:

**9 << 5 ≈ 6 ≈ 7 ≈ 8 < 12 < 2 ≈ 3 ≈ 4 < 1 < 10 << 11**

Nitrone **11** shows highest interaction energy of –486.126 kJ/mol and nitrone **9** shows the least interaction energy of -367.806 kJ/mol along the series. The interaction energies of nitrones **2**, **3** and **4** are –428.759, –425.898 and –425.673 kJ/mol respectively. These values are comparable to each other and lower than the interaction energy of **1** (= –451.802 kJ/mol). The calculated interaction energies for nitrones **5**, **6**, **7** and **8** are –402.485, –396.124, –400.309 and –402.485 kJ/mol respectively. It should be noted in this context that the calculated interaction energy trends show a definite pattern on the basis of substituent attached to the *C*-phenyl group of the reacting nitrone. Nitrones **2**, **3** and **4** involve a lactobionyl moiety attached to the aromatic ring of PBN and they show comparable interaction energies. Nitrones **5**, **6**, **7** and **8** have the *p*-carboxylate group as the *C*-phenyl substituent and show comparable energies. Nitrones **9**, **10**, **11** and **12** have different aromatic substituents and therefore show different ranges of interaction energies. When we compare nitrones **9** and **11**, it is evident that the presence of phosphorous substitution results in considerable lowering of 118.320 kJ/mol in the global interaction energy. Nitrones **9** and **12** with substituted phosphorous and nitrogen groups as the *C*-phenyl substituents show the highest values of $\Delta E_\upsilon$ of –4.967 kJ/mol and -6.335 kJ/mol respectively. However, the other nitrones show $\Delta E_\upsilon$ values of less than **1** along the series. This further indicates greater energy changes at constant external potential for nitrones **9** and **12** during the radical attacks.

Now, let us analyze the calculations from local viewpoint. The interaction energy $(\Delta E_{int})^k_{dipole}$ will be dominated by the local properties of the carbon and oxygen atoms of the nitrone. $\Delta E_\upsilon$ and $\Delta E'_\mu$ are negative in all cases and $\Delta E'_\mu$ larger in absolute value than the $\Delta E_\upsilon$ terms. These are collected in Table 3. From the electronic chemical potential values (Table 1), the direction of charge transfer is predicted from nitrones **1**-**8**, **10** and **11** to the radical. Therefore, electrophilic attack to the radical is considered. The calculated local interaction energies for electrophilic attack at C3of nitrones **1**-**8**, **10** and **11** is greater than that at O1 of these nitrones (Table 3) from both NPA and MK analyses. The difference between these local interaction energies for electrophilic attack at C3 and O1 of the nitrones **1**-**8**, **10** and **11** range from 94.742 to 150.461 kJ/mol from NPA analysis and 22.772 to 122.299 kJ/mol from MK analysis. The local interaction energy for electrophilic attack at C3 of nitrone **11** calculated as -988.743 kJ/mol is the highest value along the series. This is in conformity with the highest global interaction energy of nitrone **11**. The electronic chemical potential values and global electrophilicity indices further indicate charge transfer from the radical to nitrones **9** and **12**. Therefore, nucleophilic attack to the nitrone is to be considered. The calculated local interaction energies for nucleophilic attacks at C3 for nitrones **9** and **12** are greater than that at O1 of the nitrone (Table 3). Experimentally, radical attack to nitrones takes place at C3. This indicates that the local interaction energies provide correct interpretation for the radical attack at these nitrones.

Table 3—Interaction energies (in kJ/mol) for global-global and local-global interactions of nitrones **1**-**12** to methyl radical

| $\Delta E$ | Global-global interactions | Natural population analysis (NPA) | | | | Merz-Kollman (MK) | | | |
|---|---|---|---|---|---|---|---|---|---|
| | | Nucleophilic attack at atom | | Electrophilic attack at atom | | Nucleophilic attack at atom | | Electrophilic attack at atom | |
| | | O1 | C3 | O1 | C3 | O1 | C3 | O1 | C3 |
| **1**+$CH_3^{\cdot}$ | | | | | | | | | |
| $\Delta E_\upsilon$ | -0.530 | -0.138 | -0.142 | -0.262 | -0.163 | -0.170 | -0.310 | -0.232 | -0.190 |
| $\Delta E'_\mu$ | -451.272 | -941.039 | -936.341 | -786.078 | -909.107 | -900.377 | -726.480 | -824.592 | -876.921 |
| IE | $\Delta E_{int}$ | | | | $(\Delta E_{int})^k$ | | | | |
| | -0.530-451.272λ | -0.138-941.039λ | -0.142-936.341λ | -0.262-786.078λ | -0.163-909.107λ | -0.170-900.377λ | -0.310-726.480λ | -0.232-824.592λ | -0.190-876.921λ |
| **2**+$CH_3^{\cdot}$ | | | | | | | | | |
| $\Delta E_\upsilon$ | -0.595 | -0.146 | -0.145 | -0.254 | -0.160 | -0.180 | -0.319 | -0.225 | -0.206 |
| $\Delta E'_\mu$ | -428.164 | -945.785 | -946.467 | -821.496 | -929.052 | -905.970 | -745.881 | -853.544 | -876.335 |
| IE | $\Delta E_{int}$ | | | | $(\Delta E_{int})^k$ | | | | |
| | -0.595-428.164λ | -0.146-945.785λ | -0.145-946.467λ | -0.254-821.496λ | -0.160-929.052λ | -0.180-905.970λ | -0.319-745.881λ | -0.225-853.544λ | -0.206-876.335λ |
| **3**+$CH_3^{\cdot}$ | | | | | | | | | |
| $\Delta E_\upsilon$ | -0.647 | -0.158 | -0.158 | -0.246 | -0.157 | -0.190 | -0.330 | -0.218 | -0.192 |
| $\Delta E'_\mu$ | -425.251 | -945.104 | -945.104 | -851.882 | -946.467 | -911.632 | -761.898 | -881.040 | -909.107 |
| IE | $\Delta E_{int}$ | | | | $(\Delta E_{int})^k$ | | | | |
| | -0.647-425.251λ | -0.158-945.104λ | -0.158-945.104λ | -0.246-851.882λ | -0.157-946.467λ | -0.190-911.632λ | -0.330-761.898λ | -0.218-881.040λ | -0.192-909.107λ |
| **4**+$CH_3^{\cdot}$ | | | | | | | | | |
| $\Delta E_\upsilon$ | -0.422 | -0.094 | -0.099 | -0.170 | -0.103 | -0.114 | -0.206 | -0.151 | -0.129 |
| $\Delta E'_\mu$ | -425.251 | -959.613 | -951.958 | -836.146 | -945.104 | -927.083 | -777.695 | -867.647 | -902.854 |
| IE | $\Delta E_{int}$ | | | | $(\Delta E_{int})^k$ | | | | |
| | -0.422-425.251λ | -0.094-959.613λ | -0.099-951.958λ | -0.170-836.146λ | -0.103-945.104λ | -0.114-924.083λ | -0.206-777.695λ | -0.151-867.647λ | -0.129-902.854λ |
| **5**+$CH_3^{\cdot}$ | | | | | | | | | |
| $\Delta E_\upsilon$ | -0.048 | -0.006 | -0.003 | -0.023 | -0.013 | -0.012 | -0.027 | -0.020 | -0.014 |
| $\Delta E'_\mu$ | -402.437 | -1020.008 | -1073.385 | -782.797 | -925.123 | -941.714 | -714.616 | -823.557 | -904.098 |
| IE | $\Delta E_{int}$ | | | | $(\Delta E_{int})^k$ | | | | |
| | -0.048-402.437λ | -0.006-1020.008λ | -0.003-1073.385λ | -0.023-782.797λ | -0.013-925.123λ | -0.012-941.714λ | -0.027-714.616λ | -0.020-823.557λ | -0.014-904.098λ |
| **6**+$CH_3^{\cdot}$ | | | | | | | | | |
| $\Delta E_\upsilon$ | -0.121 | -0.013 | -0.008 | -0.056 | -0.030 | -0.018 | -0.065 | -0.048 | -0.027 |
| $\Delta E'_\mu$ | -396.003 | -1034.476 | -1062.955 | -781.864 | -932.351 | -1005.939 | -725.677 | -830.329 | -952.649 |
| IE | $\Delta E_{int}$ | | | | $(\Delta E_{int})^k$ | | | | |
| | -0.121-396.003λ | -0.013-1034.476λ | -0.008-1062.955λ | -0.056-781.864λ | -0.030-932.351λ | -0.018-1005.939λ | -0.065-725.677λ | -0.048-830.329λ | -0.027-952.649λ |
| **7**+$CH_3^{\cdot}$ | | | | | | | | | |
| $\Delta E_\upsilon$ | -0.080 | -0.009 | -0.006 | -0.038 | -0.022 | -0.014 | -0.040 | -0.034 | -0.026 |
| $\Delta E'_\mu$ | -400.229 | -1036.109 | -1062.095 | -774.941 | -918.649 | -987.030 | -761.898 | -815.373 | -878.681 |
| IE | $\Delta E_{int}$ | | | | $(\Delta E_{int})^k$ | | | | |
| | -0.080-400.229λ | -0.009-1036.109λ | -0.006-1062.095λ | -0.038-774.941λ | -0.022-918.649λ | -0.014-987.030λ | -0.040-761.898λ | -0.034-815.373λ | -0.026-878.681λ |

*(Contd.)*

Table 3—Interaction energies (in kJ/mol) for global-global and local-global interactions of nitrones 1-12 to methyl radical *(Contd.)*

| $\Delta E$ | Global-global interactions | Natural population analysis (NPA) | | | | Merz-Kollman (MK) | | | |
|---|---|---|---|---|---|---|---|---|---|
| | | Nucleophilic attack at atom | | Electrophilic attack at atom | | Nucleophilic attack at atom | | Electrophilic attack at atom | |
| | | O1 | C3 | O1 | C3 | O1 | C3 | O1 | C3 |
| **8**+$CH_3^{\cdot}$ | | | | | | | | | |
| $\Delta E_\upsilon$ | -0.048 | -0.006 | -0.003 | -0.022 | -0.013 | -0.011 | -0.022 | -0.019 | -0.015 |
| $\Delta E'_\mu$ | -402.437 | -1023.188 | -1073.385 | -787.965 | -921.228 | -953.341 | -790.813 | -829.280 | -888.795 |
| IE | $\Delta E_{int}$ | | | | $(\Delta E_{int})^k$ | | | | |
| | -0.048-402.437λ | -0.006-1023.188λ | -0.003-1073.385λ | -0.022-787.965λ | -0.013-921.228λ | -0.011-953.341λ | -0.022-790.813λ | -0.019-829.280λ | -0.015-888.795λ |
| **9**+$CH_3^{\cdot}$ | | | | | | | | | |
| $\Delta E_\upsilon$ | -4.967 | -0.179 | -0.120 | -2.570 | -1.664 | -0.164 | -0.135 | -2.290 | -1.876 |
| $\Delta E'_\mu$ | -362.839 | -1086.714 | -1094.871 | -724.876 | -861.950 | -1088.516 | -1093.047 | -767.241 | -830.329 |
| IE | $\Delta E_{int}$ | | | | $(\Delta E_{int})^k$ | | | | |
| | -4.967-362.839λ | -0.179-1086.714λ | -0.120-1094.871λ | -2.570-724.876λ | -1.664-861.950λ | -0.164-1088.516λ | -0.135-1093.047λ | -2.290-767.241λ | -1.876-830.329λ |
| **10**+$CH_3^{\cdot}$ | | | | | | | | | |
| $\Delta E_\upsilon$ | -0.906 | -0.226 | -0.244 | -0.401 | -0.226 | -0.274 | -0.494 | -0.356 | -0.252 |
| $\Delta E'_\mu$ | -435.118 | -944.424 | -930.369 | -812.848 | -944.424 | -907.849 | -743.768 | -846.935 | -924.472 |
| IE | $\Delta E_{int}$ | | | | $(\Delta E_{int})^k$ | | | | |
| | -0.906-435.118λ | -0.226-944.424λ | -0.244-930.369λ | -0.401-812.848λ | -0.226-944.424λ | -0.274-907.849λ | -0.494-743.768λ | -0.356-846.935λ | -0.252-924.472λ |
| **11**+$CH_3^{\cdot}$ | | | | | | | | | |
| $\Delta E_\upsilon$ | -0.462 | -0.115 | -0.178 | -0.183 | -0.092 | -0.122 | -0.262 | -0.150 | -0.116 |
| $\Delta E'_\mu$ | -485.664 | -957.513 | -871.102 | -863.651 | -988.517 | -947.150 | -757.939 | -909.737 | -955.422 |
| IE | $\Delta E_{int}$ | | | | $(\Delta E_{int})^k$ | | | | |
| | -0.462-485.664λ | -0.115-957.513λ | -0.178-871.102λ | -0.183-863.651λ | -0.092-988.517λ | -0.122-947.150λ | -0.262-757.939λ | -0.150-909.737λ | -0.116-955.422λ |
| **12** + $CH_3^{\cdot}$ | | | | | | | | | |
| $\Delta E_\upsilon$ | -6.335 | -1.518 | -0.687 | -1.630 | -1.568 | -1.809 | -2.244 | -1.325 | -1.204 |
| $\Delta E'_\mu$ | -401.330 | -943.068 | -1036.109 | -930.369 | -937.009 | -909.737 | -991.385 | -964.548 | -978.204 |
| IE | $\Delta E_{int}$ | | | | $(\Delta E_{int})^k$ | | | | |
| | -6.335-401.330λ | -1.518-943.068λ | -0.687-1036.109λ | -1.630-930.369λ | -1.568-937.009λ | -1.809-909.737λ | -2.244-991.385λ | -1.325-964.548λ | -1.204-978.204λ |

[a]Calculated from Eqs (4) and (5); IE: Interaction energy

**Reaction energies and hyperfine splitting constants of adducts**

The reaction energies of *cis* and *trans* radical adducts of nitrones **1**-**12** have been listed in Table 4. To model these systems more accurately, computational solution models are needed. Therefore, solvent effects (in water) were considered on the basis of single point energy calculations at the gas phase DFT/B3LYP/6-31G(d) optimized geometries from polarized continuum model[41,42]. The **1**-Me (*cis*) radical adduct is stabilized by only 3.120 kJ/mol in gas phase and by 1.903 kJ/mol in water compared to the **1**-Me (*trans*) radical adduct. However, the *cis* adducts of nitrones **2**, **3**, **4**, **5**, **6**, **7**, **8**, **9** and **12** are stabilized respectively by 19.602, 16.312, 14.689, 19.198, 18.263, 19.022, 14.590, 16.525 and 18.224 kJ/mol in water compared to the respective *trans* adducts. The *cis* adducts for nitrones **10** and **11** are stabilized than their *trans* adducts by 32.874 and 57.216 kJ/mol in water. These data suggest that nitrogen and *C*-aryl substitution has pronounced effect on the stability of radical adducts for the investigated nitrone series. The difference between *cis* and *trans* radical adducts of nitrones **2**-**9** are comparable to each other. Nitrones **5** and **10** have similar nitrogen substituents. However, the change of *C*-aryl substitution from *p*-COONa in **5** to

Table 4—Bond distances, bond orders, reaction energies $\Delta E_{reaction}$ and hyperfine splitting constants of DFT/B3LYP/6-31G(d) optimized nitrones and nitrone-radical adducts

| Comp. | Bond distances (Å) | | | Wiberg bond index | | | $\Delta E_{reaction}$ (kJ mol$^{-1}$)[a] | $\Delta E_{reaction}$ (kJ mol$^{-1}$)[b] | $\alpha_H$ (mT) | |
|---|---|---|---|---|---|---|---|---|---|---|
| | NO | CN | CC | NO | CN | CC | | | Calc.[c] | Expt.[11] |
| **1** | 1.279 | 1.317 | – | 1.2841 | 1.4692 | – | – | – | – | |
| **1**-$CH_3$ (*cis*) | 1.286 | 1.485 | 1.535 | 1.2898 | 0.9283 | 0.9992 | −178.138 | −172.025 | 0.275 | 0.368 |
| **1**-$CH_3$ (*trans*) | 1.285 | 1.481 | 1.537 | 1.2896 | 0.9310 | 0.9967 | −175.018 | −170.122 | 0.231 | |
| **2** | 1.280 | 1.317 | – | 1.2824 | 1.4637 | – | – | – | – | |
| **2**-$CH_3$ (*cis*) | 1.286 | 1.486 | 1.535 | 1.2877 | 0.9265 | 0.9989 | −178.474 | −173.892 | 0.265 | 0.388 |
| **2**-$CH_3$ (*trans*) | 1.289 | 1.498 | 1.533 | 1.2844 | 0.9218 | 1.0123 | −158.444 | −154.290 | 0.076 | |
| **3** | 1.280 | 1.316 | – | 1.2806 | 1.4706 | – | – | – | – | |
| **3**-$CH_3$ (*cis*) | 1.285 | 1.483 | 1.537 | 1.2900 | 0.9308 | 0.9966 | −176.854 | −174.070 | 0.353 | 0.394 |
| **3**-$CH_3$ (*trans*) | 1.289 | 1.494 | 1.536 | 1.2857 | 0.9277 | 1.0066 | −158.756 | −157.758 | 0.096 | |
| **4** | 1.281 | 1.316 | – | 1.2776 | 1.4703 | – | – | – | – | |
| **4**-$CH_3$ (*cis*) | 1.285 | 1.487 | 1.535 | 1.2913 | 0.9249 | 0.9985 | −168.817 | −163.466 | 0.218 | 0.385 |
| **4**-$CH_3$ (*trans*) | 1.289 | 1.498 | 1.533 | 1.2872 | 0.9213 | 1.0118 | −154.511 | −148.777 | 0.045 | |
| **5** | 1.287 | 1.315 | – | 1.2629 | 1.4746 | – | – | – | – | – |
| **5**-$CH_3$ (*cis*) | 1.288 | 1.481 | 1.536 | 1.2831 | 0.9300 | 0.9967 | −180.621 | −174.055 | 0.197 | |
| **5**-$CH_3$ (*trans*) | 1.292 | 1.503 | 1.540 | 1.2787 | 0.9074 | 0.9883 | −160.644 | −154.857 | 0.071 | |
| **6** | 1.286 | 1.315 | – | 1.2593 | 1.4735 | – | – | – | – | |
| **6**-$CH_3$ (*cis*) | 1.286 | 1.498 | 1.544 | 1.2864 | 0.9106 | 0.9821 | −175.953 | −171.471 | 0.350 | 0.373 |
| **6**-$CH_3$ (*trans*) | 1.289 | 1.498 | 1.533 | 1.2837 | 0.9205 | 1.0116 | −155.422 | −153.208 | 0.052 | |
| **7** | 1.281 | 1.317 | – | 1.2751 | 1.4643 | – | – | – | – | – |
| **7**-$CH_3$ (*cis*) | 1.285 | 1.490 | 1.534 | 1.2929 | 0.9222 | 1.0001 | −186.668 | −176.796 | 0.254 | |
| **7**-$CH_3$ (*trans*) | 1.290 | 1.498 | 1.533 | 1.2833 | 0.9198 | 1.0114 | −168.544 | −157.774 | 0.042 | |
| **8** | 1.284 | 1.317 | – | 1.2712 | 1.4627 | – | – | – | – | – |
| **8**-$CH_3$ (*cis*) | 1.286 | 1.490 | 1.534 | 1.2897 | 0.9223 | 1.0006 | −183.431 | −169.723 | 0.244 | |
| **8**-$CH_3$ (*trans*) | 1.290 | 1.494 | 1.535 | 1.2827 | 0.9234 | 1.0073 | −160.691 | −155.133 | 0.068 | |
| **9** | 1.278 | 1.317 | – | 1.2903 | 1.4686 | – | – | – | – | – |
| **9**-$CH_3$ (*cis*) | 1.285 | 1.481 | 1.538 | 1.2897 | 0.9318 | 0.9947 | −169.875 | −166.622 | 0.092 | |
| **9**-$CH_3$ (*trans*) | 1.288 | 1.492 | 1.535 | 1.2862 | 0.9296 | 1.0073 | −147.456 | −150.097 | 0.079 | |
| **10** | 1.285 | 1.317 | – | 1.2635 | 1.4692 | – | – | – | – | – |
| **10**-$CH_3$ (*cis*) | 1.286 | 1.490 | 1.536 | 1.2905 | 0.9188 | 0.9995 | −181.797 | −169.284 | 0.325 | |
| **10**-$CH_3$ (*trans*) | 1.289 | 1.507 | 1.534 | 1.2879 | 0.9119 | 1.0127 | −147.818 | −136.410 | 0.028 | |
| **11** | 1.278 | 1.317 | – | 1.2844 | 1.4849 | – | – | – | – | – |
| **11**-$CH_3$ (*cis*) | 1.286 | 1.484 | 1.535 | 1.2874 | 0.9309 | 0.9979 | −213.138 | −208.342 | 0.322 | |
| **11**-$CH_3$ (*trans*) | 1.293 | 1.499 | 1.543 | 1.2692 | 0.9299 | 0.9969 | −205.944 | −151.126 | 0.269 | |
| **12** | 1.268 | 1.321 | – | 1.3322 | 1.4495 | – | – | – | – | – |
| **12**-$CH_3$ (*cis*) | 1.283 | 1.483 | 1.536 | 1.2946 | 0.9276 | 0.9962 | −173.637 | −165.761 | 0.139 | |
| **12**-$CH_3$ (*trans*) | 1.287 | 1.493 | 1.534 | 1.2887 | 0.9276 | 1.0085 | −151.187 | −147.537 | 0.058 | |

[a]B3LYP/6-31G(d); [b]PCM/B3LYP/6-31G(d)//B3LYP/6-31G(d).
[c]Calculated by PCM/B3LYP/6-31G(d)//B3LYP/6-31G(d).

*o*-$OCH_2CH_3$ in **10** results in the increased stability difference by 13.676 kJ/mol. Nitrones **9** and **11** have similar nitrogen substituents. However, the change of *C*-aryl substitution from *p*-$OCH_2CH_2P(Ph_3)$ in **9** to *p*-$OC_{12}H_{25}$ and *m*-$OC_6H_{12}COO(CH_2NMe_3)(CH_2COOC_8H_{17})$ in **11** as the *C*-aryl substituents increases the stability difference by 40.691 kJ/mol. This implies that the O-alkyl substitution of the *C*-aryl ring increases the stability differences in this series. The calculated bond distances and bond orders of the nitrones and radical adducts are listed in Table 4. C-N bond distances of the *cis* and *trans* adducts show values in the range 1.499 to 1.481 Å. The wiberg bond order values for the nitrone C-N bond in the range 1.47-1.45 are changed to the range 0.92-0.93 in the radical adducts. PCM/B3LYP/6-31G(d)//B3LYP/6-31G(d) calculated hyperfine splitting constants are listed in Table 4. The experimental values for the methyl radical adducts of nitrones **1**, **2**, **3**, **4** and **6** are available in literature. $\alpha_H$ values for the *cis* adducts are comparable to the experimental data. For instance, the calculated $\alpha_H$

values for 3-Me (*cis*) and 6-Me (*cis*) adduct are 0.353 and 0.350 and the reported experimental values are 0.394 and 0.373 respectively. However, the calculated $\alpha_H$ values for 3-Me (*trans*) and 6-Me (*trans*) adduct are 0.096 and 0.052 respectively. These values further suggest the stability of *cis* adduct compared to the *trans* adduct in conformity with the reaction energies.

**Transition states**

Nitrones **1**, **5**, **6**, **8**, **9** and **12** have been selected as the cost effective computational models for the location of transition states during the study. Total 12 transition states corresponding to *cis* and *trans* methyl radical attacks to the nitrones were successfully located at DFT/B3LYP/6-31G(d) level of theory. The optimized transition state geometries are shown in Fig. 3. The Wiberg bond indices and atom-atom overlap weighted NAO bond orders were calculated to examine the extent of bond formation in the transition states (Table 5). Nitrone-Me (*trans*) transition states show lower forming C-C bond order

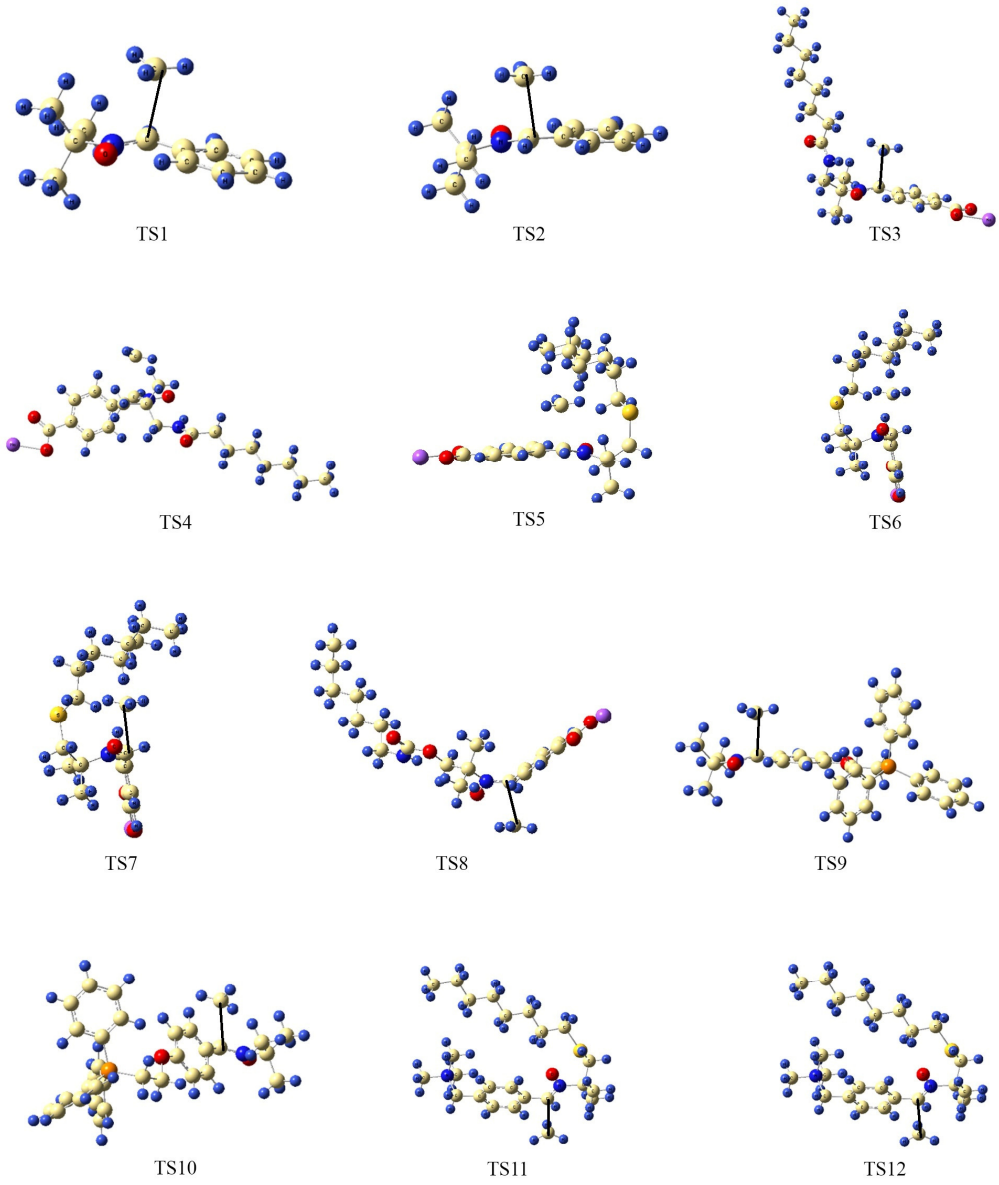


Fig. 3—DFT/B3LYP/6-31G(d) optimized transition states.

Table 5—Bond distances, bond orders and activation energies of transition states

| Comp. | Bond distances (Å) | | | Atom-atom overlap-weighted NAO bond order | | | Wiberg bond index | | | $E^{\#}$ (kJ mol$^{-1}$) | |
|---|---|---|---|---|---|---|---|---|---|---|---|
| | N-O | C-N | C- C | N-O | C-N | C- C | N-O | C-N | C-C | B3LYP/ 6-31G(d) | PCM/B3LYP/ 6-31G(d)// B3LYP/6-31G(d) |
| TS1[**1**-$CH_3$ (*cis*)] | 1.282 | 1.335 | 2.496 | 0.9426 | 1.0909 | 0.1515 | 1.2791 | 1.3652 | 0.1867 | 13.452 | 15.812 |
| TS2 [**1**-$CH_3$ (*trans*)] | 1.282 | 1.335 | 2.495 | 0.9424 | 1.0908 | 0.1519 | 1.2790 | 1.3649 | 0.1872 | 13.453 | 15.854 |
| TS3 [**5**-$CH_3$ (*cis*)] | 1.288 | 1.334 | 2.489 | 0.9331 | 1.0951 | 0.1541 | 1.2628 | 1.3738 | 0.1896 | 14.234 | 15.539 |
| TS4 [**5**-$CH_3$ (*trans*)] | 1.296 | 1.330 | 2.579 | 0.9127 | 1.1197 | 0.1310 | 1.2425 | 1.4463 | 0.1688 | 57.283 | 64.037 |
| TS5 [**6**-$CH_3$ (*cis*)] | 1.286 | 1.335 | 2.496 | 0.9334 | 1.0938 | 0.1522 | 1.2610 | 1.3711 | 0.1912 | 18.989 | 20.798 |
| TS6 [**6**-$CH_3$ (*trans*)] | 1.288 | 1.329 | 2.597 | 0.9297 | 1.1202 | 0.1232 | 1.2616 | 1.4510 | 0.1642 | 67.394 | 68.085 |
| TS7 [**8**-$CH_3$ (*cis*)] | 1.286 | 1.335 | 2.494 | 0.9350 | 1.0903 | 0.1520 | 1.2679 | 1.3653 | 0.1877 | 11.866 | 15.294 |
| TS8 [**8**-$CH_3$ (*trans*)] | 1.292 | 1.335 | 2.550 | 0.9251 | 1.1041 | 0.1330 | 1.2610 | 1.4155 | 0.1686 | 55.466 | 59.873 |
| TS9 [**9**-$CH_3$ (*cis*)] | 1.282 | 1.335 | 2.495 | 0.9437 | 1.0895 | 0.1527 | 1.2830 | 1.3636 | 0.1886 | 14.129 | 17.362 |
| TS10 [**9**-$CH_3$ (*trans*)] | 1.280 | 1.335 | 2.613 | 0.9478 | 1.1018 | 0.1213 | 1.3009 | 1.4115 | 0.1574 | 59.609 | 59.095 |
| TS11 [**12**-$CH_3$ (*cis*)] | 1.280 | 1.335 | 2.510 | 0.9507 | 1.0873 | 0.1473 | 1.2926 | 1.3607 | 0.1813 | 6.910 | 14.138 |
| TS12 [**12**-$CH_3$ (*trans*)] | 1.281 | 1.338 | 2.600 | 0.9471 | 1.0960 | 0.1252 | 1.2976 | 1.3999 | 0.1622 | 69.898 | 67.955 |

values compared to the corresponding *cis* channel for nitrones **5**, **6**, **8**, **9** and **12**. The Wiberg bond indices and atom-atom overlap weighted NAO bond orders of C-C forming bond in the *cis* and *trans* radical adducts are respectively calculated in the range 0.98–1.01 and 0.83–0.85. For the transition states, these bond orders account to 0.15–0.19 and 0.12–0.15 respectively leading to the formation of *cis* and *trans* adducts. On the other hand, the forming C-N bond orders in the transition states of *cis* adducts are lower than the *trans* adducts of these nitrones. The forming C-C bond lengths in the *cis* adduct transition states are shorter than the *trans* adducts. These data overall suggest the favored generation of *cis* radical adducts. This is in complete agreement with the computed reaction energies listed in Table 4. The bond order and bond length values for the *cis* and *trans* adducts of nitrone **1** are comparable and is also in conformity with their calculated reaction energies (Table 4).

The *trans* adducts show higher activation energies than the corresponding *cis* adducts both in gas phase and water for the nitrones **5**, **6**, **8, 9** and **12**. The activation energies of TS3-TS4, TS5-TS6, TS7-TS8, TS9-TS10 and TS11-TS12 transition state pairs differ by 43.049, 48.405, 43.600, 45.480 and 62.988 kJ/mol respectively from gas phase calculations. The corresponding differences account to 48.498, 47.287, 42.511, 41.733 and 53.817 kJ/mol in water. Inclusion of solvent effects resulted to enhanced activation barrier in each case. On the other hand, the activation energies for the *cis* and *trans* adduct formations of nitrone **1** are comparable to each other (15.812 kJ/mol and 15.854 kJ/mol respectively in water). This implies that substitution increases the stability of the *cis* adduct.

## Conclusions

The α-phenyl-*N*-*t*-butyl nitrone derivatives show varied electron demand characteristics with the change of nitrogen and aryl substitutions which determines their charge transfer directions during the methyl radical capture by these nitrones. Introduction of $PPh_3$and $NMe_3$ groups in the *C*- phenyl substituent chain of the nitrone increases the electrophilicity of these nitrones. DFT based local reactivity indices calculated from MK calculations perform better than the NPA system to rationalize the site of radical attack. The calculated interaction energies show a definite pattern on the basis of substituent attached to the *C*-phenyl group of the reacting nitrone. Greater interaction energy changes at constant external potential are predicted for $PPh_3$ and $NMe_3$ substituted nitrones during the radical attacks. The local interaction energies provide correct interpretation (C3 attack) for the radical capture. Preferred generation of *cis* adduct is predicted from forming bond orders at the transition states, computed reaction energies, activation energies and hyperfine splitting constants which is in complete agreement with the reported experimental

results. Both nitrogen and C-aryl substitutions at the nitrone increase the stability difference of the *cis* and *trans* radical attacks.

## Supplementary Data

Supplementary data associated with this article, i. e., Tables S1-S96, are available in the electronic form at http://www.niscair.res.in/jinfo/ijca/IJCA_56A(01)9-20_SupplData.pdf.

## References


1 Sen S & J W Phillis J A, *Free Radic Res Commun*, 19 (1993) 255.
2 Floyd R A, *Free Radic Biol Med*, 46 (2009) 1004.
3 Floyd R A, Hensley K, Forster M J, Kelleher-Andersson J A & Wood P L, *Mech. Ageing Dev*, 30 (2002) 1021.
4 Floyd R A, Hensley K, Forster M J, Kelleher-Andersson J A & Wood P L, *Ann NY Acad Sci*, 959 (2002) 321.
5 Liu J, Atamna H, Kuratsune H & Ames B N, *Ann NY Acad Sci*, 959 (2002) 133.
6 Atamna H, Paler-Martínez A & Ames B N, *J Biol Chem*, 275 (2000) 6741.
7 Novakov C P & Stoyanovsky D A, *Chem Res Toxicol*, 15 (2002) 749.
8 Janzen E G, Dudley R L & Shetty R V, *J Am Chem Soc*, 101 (1979) 243.
9 Marshall J W B, Duffin K J, Green A R & Ridley R M, Stroke, 32 (2001) 190.
10 Dhainaut A, Tizot A, Raimbaud E, Lockhart B, Lestage P & Goldstein S, *J Med Chem*, 43 (2000) 2165.
11 Durand G, Polidori A, Ouari O, Tordo P, Geromel V, Rustin P & Pucci B, *J Med Chem*, 46 (2003) 5230.
12 Durand G, Poeggeler B, Boker J, Raynal S, Polidori A, Pappolla M A, Hardeland R & Pucci B, *J Med Chem*, 50 (2007) 3976.
13 Murphy M P, Echtay K S, Blaikie F H, Asin-Cayuela J, Cocheme´ H M, Green K, Buckingham J A, Taylor E R, Hurrell F, Hughes G, Miwa S, Cooper C E, Svistunenko D A, Smith R A J & Brand M D, *J Biol Chem*, 278 (2003) 48534.
14 Reddy P H, *J Biomed Biotechnol*, 2006, Article ID 31372, 1.
15 Navarro A & Boveris A, *Adv Drug Del Rev*, 60 (2008) 1534.
16 Fangour S El, Marini M, Good J, McQuaker S J, Shiels P G & Hartley R C**,** *AGE*, 31 (2009) 269.
17 Parr R G & Yang W, *Density Functional Theory of Atoms and Molecules,* (Oxford University Press, NewYork) 1989.
18 Geerlings P, Proft F De & Langenaeker W, *Chem Rev*, 103 (2003) 1793.
19 Chermette H, *J Comput Chem*, 20 (1999) 129.
20 Parr R G & Pearson R G, *J Am Chem Soc*, 105 (1983) 7512.
21 Chattaraj P K, Sarkar U & Roy D R, *Chem Rev*, 106 (2006) 2065.
22 Reed A E & Weinhold F, *J Chem Phys*, 78 (1983) 4066.
23 Besler B H, Merz Jr K M & Kollman P A, *J Comput Chem*, 11 (1990) 431.
24 Domingo L R, Sáez J A & Pérez P, *Chem Phys Lett*, 438 (2007) 341.
25 Benchouk W & Mekelleche S M, *J Mol Struct: THEOCHEM*, 852 (2008) 46.
26 Yang W & Mortier W J, *J Am Chem Soc*, 108 (1986) 5708.
27 Chandra A K & Nguyen M T, *J Chem Soc, Perkin Trans,* 2 (1997) 1415.
28 Méndez F, Tamariz J & Geerlings P, *J Phys Chem A,* 102 (1998) 6292.
29 Parr R G & Gázquez J L, *J Phys Chem*, 97 (1993) 3939.
30 Gázquez J L, Martinez A & Méndez F, *J Phys Chem* 97 (1993) 4059.
31 Gázquez J L, *Chemical Hardness-Structure and Bonding,* Vol. 80, edited by K D Sen & D M P Mingos, (Springer, New York), 1993, p. 27.
32 Becke A D, *J Chem Phys*, 98 (1993) 5648.
33 Lee C, Yang W & Parr R G, *Phys Rev B*, 37 (1988) 785.
34 *Gaussian 03, Rev. D.01* (Gaussian, Inc., Wallingford CT) 2004.
35 Domingo L R, Aurell M J, Pe´rez P & Contreras R, *Tetrahedron*, 58 (2002) 4417.
36 Nguyen H M T, Peeters J, Nguyen M T & Chandra A K, *J Phys Chem A*, 108 (2004) 484.
37 Ponti A, *J Phys Chem A*, 104 (2000) 8843.
38 Mendez F & Garcia-Garibay M A, *J Org Chem*, 64 (1999) 7061.
39 Acharjee N, *J Theoret Comput Chem*, 13 (2014) 1450071.
40 Acharjee N, *J Theoret Comput Chem*, 13 (2014) 1450007.
41 Miertus S & Tomasi J, *Chem Phys*, 65(1982) 239.
42 Barone V & Cossi M, *J Phys Chem A*, 102 (1998) 1995.